Anal. Chem. **2002,** *74,* 570−576

Ketocyanine Dyes: H^+-Selective Ionophores for Use in Integrated Waveguides Absorbance Optodes

Mar Puyol, Serguei Miltsov, Íñigo Salinas,† and Julian Alonso*

Sensors & Biosensors Group, Department of Chemistry, Autonomous University of Barcelona, Edifici Cn, 08193 Bellaterra, Catalonia, Spain

The optical and analytical characteristics of a series of neutral H^+-selective chromoionophores in PVC membranes are described. Such indicators have been synthesized so that they can operate in bulk optode membranes as the chemically active region of integrated waveguide absorbance optodes (IWAOs), λ_{max} near 780 nm. Their spectral characteristics, acid−base properties, chemical stability, and solubility in the membrane phase are given and discussed. The response characteristics are first tested in a conventional absorbance/transmittance flow cell. They offer a wide range of pK_a's in PVC membranes, good sensitivity as a result of their high molar absortivities, excellent solubility in the plasticizer, and quick response times. They present good chemical stability in common laboratory conditions when stored in the dark, and the absence of leaching guarantees a long lifetime. Membranes have been finally applied as the sensing region of an integrated waveguide optode, demonstrating the extraordinary sensitivity improvement while preserving the remaining analytical features. Calibration curve slopes are multiplied by 3−28, and response times lower than 2 min are obtained.

The development and application of optical sensors has become an increasingly active area of research. Most of the developed systems are based on traditional transduction phenomena as fluorescence or transmittance/absorbance, in which the selective response is accomplished by a chromoionophore that interacts with a species of interest to undergo a change in its optical properties. The most studied application has been the use of optically active pH indicators as H^+-selective ionophores to develop pH-selective optical sensors.[1−3] Another stage in the development of optical sensors has been accomplished under the leadership of Simon and co-workers. They have demonstrated the possibility of extending the set of target analytes by the generation of an indirect optical signal when combining ionic recognition mechanisms with indicator chemistry. In this way, membranes containing natural or synthetic ionophores, especially electrically neutral carriers that have been widely applied in ion-selective electrodes (ISE),[4] and acid−base indicators have paved the way for sensing chemical parameters, such as heavy metals[5] or other pollutants,[6−8] in the environment; however, new research is needed to overcome some significant limitations concerning optochemical sensing in order to reach a practical application level, especially in direct absorbance/transmittance based systems. First, optical transmission signals may be affected by light scattering or matrix absorption if light crosses the sample solution. On the other hand, optical sensors usually show long response times as a result of the intrinsic slow kinetics of mass transfer through the bulk of the membrane to reach the equilibrium, which is unfortunately worsened when thicker membranes are used to improve sensitivity. In addition, most of the reagents suffer from photobleaching or leaching.

To solve these problems, especially those related to sensitivity limitations, complex and expensive measurement setups have been used to increase the signal/noise ratio. The present work pretends to address some of these weak points. Besides increasing the dye concentration in the membrane, which is limited by its solubility in the plasticizer, there are two effective alternatives to improve sensitivity: on the one hand, changing the optically active reagent to another one with higher molar absortivity and on the other hand, increasing the optical path length. With that in mind, we first studied the optical and analytical characteristics of a series of novel neutral pH indicators, a class of ketocyanine dyes, in PVC membranes. They were synthesized[9] to present high molar absortivities and absorbance maxima in the NIR region, where simple and cheap commercially available emitting sources and detectors can be found. Second, we also proposed and demonstrated the advantages offered by an integrated waveguide absorbance optode that allows optimizing the optical path length.

† Current address: Dpto. Fisica Aplicada, Universidad de Zaragoza, Spain.

(1) Fuh, M.-R. S.; Burgess, L. W.; Hirschfeld, T.; Christian, G. D.; Wang, F. *Analyst.* **1987**, *112*, 1159−1163.
(2) Lehmann, H.; Schwotzer, G.; Czerney, P.; Mohr, G. *J. Sens. Actuators B* **1995**, *29*, 392−400.
(3) Zhang, S.; Tanaka, S.; Wickramasinghe, Y. A. B. D.; Rolfe, P. *Med. Biol. Eng. Comput.* **1995**, *33*, 152−156.
(4) Bühlmann, P.; Pretsch, E.; Bakker, E. *Chem. Rev.* **1998**, *98*, 1593−1687.
(5) Ertaş, N.; Akkaya, E. U.; Ataman, O. Y. *Talanta* **2000**, *51*, 693−699.
(6) Watanabe, K.; Nakagawa, E.; Yamada, H.; Hisamoto, H.; Suzuki, K. *Anal. Chem.* **1993**, *65*, 2704−2710.
(7) Berman, R. J.; Christian, G. D.; Burgess, L. W. *Anal. Chem.* **1990**, *62*, 2066−2071.
(8) Kawabata, Y.; Sugamoto, H.; Imasaka, T. *Anal. Chim. Acta* **1993**, *283*, 689−694.
(9) Miltsov, S.; Encinas, C.; Alonso, J. *Tetrahedron Lett.* **2001**, *42*, 6129−6131.

10.1021/ac0107960 CCC: $22.00
Published on Web 01/04/2002

It is obvious that planar waveguide chemical sensing is an extremely promising and fast-growing field.[10−13] It represents the same transduction concept as optical fibers, but with some relevant advantages assured by the IC technology, such as low-cost fabrication and mass production, easy design integration of complex waveguiding structures, and automatic membrane deposition.

The optical phenomena that provide sensing in a waveguide configuration may occur in the core layer or outside it. Most of the developed sensors involve the sensing region in the cladding, and hence, they are based in the evanescent field,[14−16] generally considered to be not very sensitive. In addition to requiring long interaction distances or a great amount of field out of the waveguide, the response strongly depends on variations of the real part of the refractive index. Core-layer-based absorbance sensors can be more sensitive, because the sensing area is probed by the major part of the energy.[17,18] The new optical concept[19,20] of the integrated device presented in this work is based on the radiation transmission through the core, which enables a light path length increase without enlarging simultaneously the membrane thickness and, hence, the response time. Moreover, interference effects from the solution matrix are minimized, because light does not interact with it.

The device consists of the same chemically active membrane as that in the conventional configuration, but it is deposited over a microfabricated planar waveguide circuit constructed using complementary metal oxide semiconductor (CMOS) compatible processes over a silicon wafer. Three regions can be differentiated in Figure 1: an input waveguide (W1), an output waveguide (W2), and the optode membrane all over them. Note that membrane covers the entire chip surface because of the deposition technique employed, but the only effective area is the region between waveguides. For a membrane thickness near 4 μm (when it exactly matches the height of the waveguide core) and membrane refractive index close to 1.46, the optical membrane works as the selective recognition region while acting as part of the light-guiding planar structure. First, light is coupled from the LED source to the input waveguide by an optical fiber, where it is guided to the open region, where the membrane is placed. Then, light remains guided through the membrane, where the absorbance/transmittance phenomena takes place as it interacts with the analyte in the sample until it reaches the output waveguide. Finally, it is coupled from the output waveguide to the detector by another optical fiber.

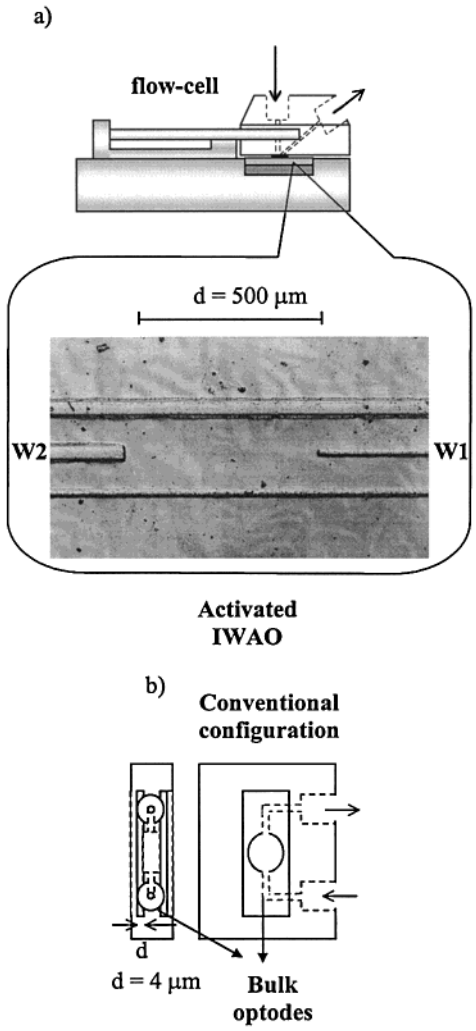

Figure 1. From left to right, the activated device in a wall-jet-layout flow cell is depicted, and an upper view of an IWAO shows the appearance of the deposited membrane, which covers the 500-μm-long cavity between the input (W1) and the output (W2) waveguides. The conventional measurement cell with a capacity of two membranes of 4 μm is also schematized.

Because the guided light path is perpendicular to the diffusion direction of the analyte through the membrane, the sensitivity depends on the optical path length, determined by the 500-μm-long cavity (defined by microelectronic techniques) and remains independent of the membrane thickness. The length of this region is chosen as a compromise between low insertion losses in the output waveguide and sensitivity.

EXPERIMENTAL SECTION

Apparatus. Conventional absorbance measurements for the PVC bulk optode characterization were performed between 830 and 400 nm by a double-beam UV−vis−NIR scanning spectrophotometer (Shimadzu UV-310PC) in a continuous-flow system using a conventional cell. The flow system was constructed with a GILSON Minipuls 3 peristaltic pump equipped with Tygon pump tubing. The flow rate used was 3 mL/min. Flow lines were built using PTFE 0.8-mm-i.d. tubing. The integrated waveguide absorbance optode (IWAO) employed in this study has a 500-μm-long cavity. To evaluate its response, another flow cell similar to a wall-

(10) Dessy, R. E.; *Anal. Chem.* **1989**, *61*, 233−240.
(11) Tóth, K.; Zagy, G.; Lau, B. T. T.; Jeney, J.; Choquette, S. J. *Anal. Chim. Acta* **1997**, *353*, 1−10.
(12) Benaisa, K.; Nathan, A. *Sens. Actuators A* **1998**, *65*, 33−44.
(13) Brecht, A.; Gauglitz, G. *Sens. Actuators B* 1997, 38−39, 1−7.
(14) Ge, Z.; Brown, C. W.; Sun, L.; Yang, S. C. *Anal. Chem.* **1993**, *65*, 2335−2338.
(15) Lee, J. E.; Saavedra, S. S. *Anal. Chim. Acta* **1994**, *285*, 265−269.
(16) Freiner, D.; Kunz, R. E.; Citterio, D.; Spichiger, U. E.; Gale, M. T. *Sens. Actuators B* **1995**, *29*, 277−285.
(17) Garcés, I.; Villuendas, F.; Subías, J.; Alonso, J.; del Valle, M.; Domínguez, C. *Opt. Lett.* **1997**, *23*, 225−227.
(18) Hisamoto, H.; Kim, K.; Manabe, Y.; Sasaki, K.; Minamitani, H.; Suzuki, K. *Anal. Chim. Acta* **1997**, *342*, 31−39.
(19) Garcés, I.; Villuendas, F.; Salinas, I.; Alonso, J.; Puyol, M.; Domínguez, C.; Llobera, A. *Sens. Actuators B* **1999**, *60*, 191−199.
(20) Puyol, M.; del Valle, M.; Garcés, I.; Villuendas, F.; Domínguez, C.; Alonso, J. *Anal. Chem.* **1999**, *71*, 5037−5044.

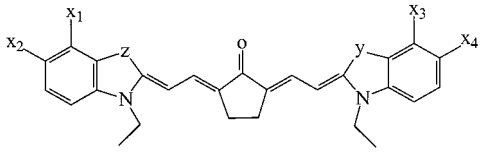

Figure 2. General structure of the unprotonated form of the tested ketocyanines.

Table 1. Chemical Structure and Identification Name of All of the Ketocyanines Tested in This Work

dye	substitutes
5aa	$X_1 = X_2 = X_3 = X_4 = H$, $Y = Z = C(CH_3)_2$
5bb	$X_1 = X_3 = H$, $X_2 = X_4 = OH$, $Y = Z = C(CH_3)_2$
5cc	$X_1 = X_3 = H$, $X_2 = X_4 = NHCOCH_3$, $Y = Z = C(CH_3)_2$
5dd	$X_1 = X_2 = X_3 = X_4 = H$, $Y = Z = S$
5ee	$X_1 + X_2 = (-CH{=}CH-)_2$, $X_3 + X_4 = (-CH{=}CH-)_2$, $Y = Z = C(CH_3)_2$
5ff	$X_1 = X_3 = OH$, $X_2 = X_4 = COOC_2H_5$, $Y = Z = C(CH_3)_2$
5ab	$X_1 = X_2 = X_3 = H$, $X_4 = OH$, $Y = Z = C(CH_3)_2$
5ac	$X_1 = X_2 = X_3 = H$, $X_4 = NCOCH_3$, $Y = Z = C(CH_3)_2$
5ad	$X_1 = X_2 = X_3 = X_4 = H$, $Y = S$, $Z = C(CH_3)_2$
5ae	$X_1 = X_2 = H$, $X_3 + X_4 = (-CH{=}CH-)_2$, $Y = Z = C(CH_3)_2$
5bc	$X_1 = X_3 = H$, $X_2 = OH$, $X_4 = NCOCH_3$, $Y = Z = C(CH_3)_2$
5bd	$X_1 = X_2 = X_3 = H$, $X_4 = OH$, $Y = C(CH_3)_2$, $Z = S$
5be	$X_1 = H$, $X_2 = OH$, $X_3 + X_4 = (-CH{=}CH-)_2$, $Y = Z = C(CH_3)_2$
5cd	$X_1 = X_2 = X_3 = H$, $X_4 = NCOCH_3$, $Y = C(CH_3)_2$, $Z = S$
5ce	$X_1 = H$, $X_2 = NHCOCH_3$, $X_3 + X_4 = (-CH{=}CH-)_2$, $Y = Z = C(CH_3)_2$
5de	$X_1 + X_2 = (-CH{=}CH-)$, $X_3 = X_4 = H$, $Y = S$, $Z = C(CH_3)_2$
7bc	$X_1 = X_3 = H$, $X_2 = OH$, $X_4 = NH_2$, $Y = Z = C(CH_3)_2$

jet layout was used. A schematic picture of both flow-cell configurations and a photographic enlargement of one of the tested sensors are depicted in Figure 1. The optical source was an LED (GCA Fiberoptics, GCA-78MI) emitting at 778 nm with 33-nm spectral width, coupling 11.26 μW optical power to the device. Fiber-emitter and fiber-detector coupling was accomplished using standard optical fiber connectors. The detector was a PIN photodiode connected to a transimpedance preamplifier. The signal was amplified and filtered using a lock-in amplifier (SR810 DSP Stanford Research Systems) that also tuned the modulation frequency of the LED source (1.1 kHz).

The pH values were determined with a glass electrode (Crison 52−03, Barcelona, Spain), and a halogen lamp (500 W) was used for the photostability study.

Reagents. All of the calibration curves were performed in a combined buffer to cover a wide pH range. It consisted of 4.0×10^{-3} M trisodium phosphate (tert) dodecahydrate (Merk, Darmstadt, Germany), 4.5×10^{-3} M sodium tetraborate decahydrate (Merk, Darmstadt, Germany), and 14.7×10^{-3} M trisodium citrate anhydrous (Carlo Erba, Milan, Italy) in doubly quartz-distilled water.

For membrane preparation, the following components were obtained from Fluka (Buchs, Switzerland): poly(vinyl chloride) (PVC high molecular weight) as the polymer, Tris(2-ethylhexyl)-phosphate (TOPH) as the plasticizer, and tetrahydrofuran (THF) as the solvent; potassium tetrakis(4-clorophenyl)borate (KTpClPB) was used as the lipophilic anionic additive, and ketocyanines (Figure 2, Table 1), as the chromoionophores.

EXPERIMENTAL SECTION

Membrane Preparation. Membrane components were weighed out and dissolved in 1.5 mL of THF to prepare the cocktail solution. The composition consisted of 0.5 wt % of the ketocyanine dye, 0.5 wt % of KTpClPB, 31.0 wt % of PVC, and 68 wt % of TOPH. To obtain membranes of 4-μm thickness, a spin-on device was used at 2000 rpm to deposit 100 μL of this cocktail over microscope slides. Another deposition technique was employed to characterize the IWAO: 50 μL of a diluted cocktail (1:2) in THF was dropped onto the device and quickly expanded over the silicon surface with the aid of a microscope slide (reproducing the screen-printing deposition technique). After THF evaporation, membranes were assumed to be near 4-μm thickness, because light guidance was completely achieved.

pK_a of Chromoionophores in Membrane. The pH response was followed in a continuous flow system. Spectra of the optical membrane were taken for each pH after the equilibrium was reached (5 min). The solution pH was varied from 3 to 8.5 by adding concentrated solutions of NaOH and HCl and was continuously monitored using a glass pH electrode.

Leaching. To ensure good sensitivity and long lifetime, reagents must be stable in the membrane phase, and hence, they should not leach. The leaching study was performed by recording the absorbance maximum of the acid or the basic form every few minutes while the membrane was continuously in contact with the buffer solution during 2 h and kept in the dark. Experiments were performed in acid (pH = 3) and basic (pH = 8) media. After that, a spectrum of the solution was taken.

Photostability of Chromoionophores. Photobleaching was studied using two experimental procedures. Membranes previously conditioned with an acid (pH = 3) or basic (pH = 8) solution were exposed to the wavelength of the absorbance maximum of the acid and the basic form. On the other hand, membranes freshly deposited onto microscope slides (always in their basic form) and kept in dry conditions were exposed to direct halogen light (500 W), placed at 150 cm. The temperature was of 23 ± 2 °C. In both experiments, membrane spectra were recorded every few minutes for 2 h. For comparison purposes, the half-life of the ketocyanine under study was calculated assuming a first-order decomposition rate and normalizing the absorbance at the recording time $t = 0$ as 100%.

Analytical Response Characteristics. To evaluate reproducibility, each membrane was subjected to pH cycles on different days. To study the response time, the absorbance maximum of the acid form was recorded with variations in pH. It was calculated as the time when 90% of the steady-state signal was reached by the fit of an exponential decay to every pH change. [20]

Sensitivity was calculated as the slope of the linear range of the calibration curve. Results obtained with the IWAO were compared to those acquired in the conventional flow-cell configuration.

RESULTS AND DISCUSSION

One of the main purposes in this work was the characterization of the optical properties of a new class of ketocyanine dyes in PVC membranes. These dyes were synthesized with the aim of procuring sensitive indicators, the absorbance maxima of which matched the wavelength of the LED employed as the light source in the integrated waveguide absorbance optode. Their synthesis and their characterization in ethanol was previously performed in our laboratory, and the results exhibit wavelengths close to 780 nm.[9] In this work, perfectly homogeneous membranes were

Table 2. Absorbance Maxima and pK_a of the Evaluated Ketocyanines in Solution and in PVC Membrane

dye	λ_{EtOH} (nm)	λ_{MEM} (nm)	pKa_{EtOH}	pKa_{MEM}[a]
5aa	717.0	735.0	2.9	7.3
5bb	747.0	766.0	≤2.1	8.4[b]
5cc	742.0	765.0	≤3.6	7.8[b]
5dd	743.0	764.0	4.3	7.9[b]
5ee	750.5	768.5	2.9	7.7
5ff	717.0	727.0	2.0	5.0
5ab	731.5	742.5	3.4	6.9
5ac	729.5	744.0	2.7	6.3
5ad	725.5	745.5	3.8	7.3
5ae	733.0	743.0	2.9	6.5
5bc	744.5	759.5	1.7	7.0
5bd	745.5	757.0	3.4	6.5
5be	748.5	766.0	3.8	8.4[b]
5cd	741.0	755.0	2.9	6.2
5ce	745.5	770.5	3.6	7.3
5de	744.0	753.0	3.3	6.5
7bc	724.0	760.0	2.7	6.9

[a] Apparent pK_a obtained from the equilibrium constant (−log Ka_{MEM}). [b] Approximated values.

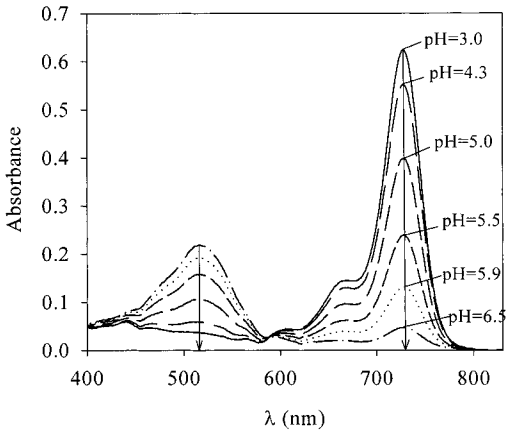

Figure 3. Absorbance spectra of ketocyanine 5ff in the TOPH-plasticized PVC membrane after equilibration with different pH-buffered solutions of the combined buffer. The excellent behavior of such class of dyes in PVC membranes can be seen. This chromoionophore shows its absorption maximum of the protonated form at 727 nm, the isosbestic point at 587 nm, and the absorption maximum of the deprotonated form at 518 nm.

prepared using each dye. They appear to be completely soluble in the organic solvent used as the plasticizer (TOPH), and no aggregation was observed during any of the experiments. All of the membrane spectra in air showed a broad band at low wavelengths so that ketocyanines were in their basic form (ketone form) in the PVC matrix; however, after doing a comparative study of the storing conditions that demonstrated an enhanced lifetime maintaining them in acid media, they were always kept in the dark and buffered at pH = 3 after each calibration.

As we expected, the absorbance maxima of ketocyanine dyes in ethanol were slightly red-shifted (longer wavelength) in the less polar solvent TOPH. Results are presented in Table 2. It is well-known that there is a large influence of solvents on absorption spectra for charged dyes (CH^+), because their conformation may change. In general, a bathochromic shift of 10−35 nm is observed, which favors the application of such cyanine class as chromoionophores in the IWAO chemically active membrane.

Membranes showed good performance during calibrations in the pH range 3−8.5. Figure 3 gives a typical example of the pH response of the ketocyanines tested. Two clear absorption peaks can be distinguished. The absorption bands related to the basic and acid forms appear in the visible region and the near infrared region, respectively. The permanency of a well-defined isosbestic point in the spectra of the immobilized indicators demonstrated that there was only one equilibrium involving two species. In a more basic media, the isosbestic point was shifted. This fact may indicate the chemical decomposition of ketocyanines at basic pH (>8.8), because no other peaks related to aggregation equilibrium were observed; however, this point does not involve a drawback, because almost all of the tested dyes are fully deprotonated at that limiting pH.

pK_a in Membrane. The evaluation of dye basicities in the membrane phase is relevant, because they will define the operational pH working range of the membrane. The apparent pK_a heavily depends on the membrane composition and mainly on the solvent mediator. Basicities were calculated from the equilibrium constant, K_{aMEM}, of each ketocyanine in the membrane phase. They were determined by fitting the experimental calibration curve to the general theoretical equation of a pH bulk optode,[21]

$$a_{H^+} = \frac{1}{Ka_{MEM}} \frac{(1-\alpha)}{\alpha} \qquad (1)$$

where α is the ratio of the dissociated form from the total amount of chromoionophore, that is, $\alpha = (A_f - A)/(A_f - A_0)$. A is the signal at any given pH, A_0 is the signal of the completely dissociated form (maximum pH), and A_f is the maximum signal of the totally protonated form (minimum pH). The calibration curve was obtained taking the absorption maximum of the acid form from the spectra when the equilibrium was reached for every pH variation between 3 and 8.5. For the more basic chromoionophores (5cc, 5dd, 5bb, 5be), a deviation of the experimental data to the ideal theoretical curve can be observed. This is attributed to their decomposition at high pH values (over pH = 8), as it has been concluded in the chemical decomposition study. For this reason, calculated pK_a's of these dyes may be approximated values. The acidity constants in the membrane phase (pK_{aMEM}) are summarized in Table 2. Note the large basicity increment for the immobilized indicators. The pK_a value increased in at least 3 pH units, which will allow working near neutral pH, and consequently, it could support widening the future application fields of the developed membranes. This can be explained by the fact that the protonated positively charged dye is stabilized to a lesser extent in the organic phase. Moreover, results reveal their suitability to develop ion-selective optodes. The response characteristics rely on the formation constant of the ionophore−analyte complex and the acidity constant of the chromoionophore in the media.[21] Therefore, for an ionophore of a specific target analyte, it is possible to select the chromoionophore that gives the best response characteristics among those synthesized (Figure 4).

(21) Bakker, E.; Bülmann, P.; Pretsch, E. *Chem. Rev.* **1997**, *97*, 3083−3132.

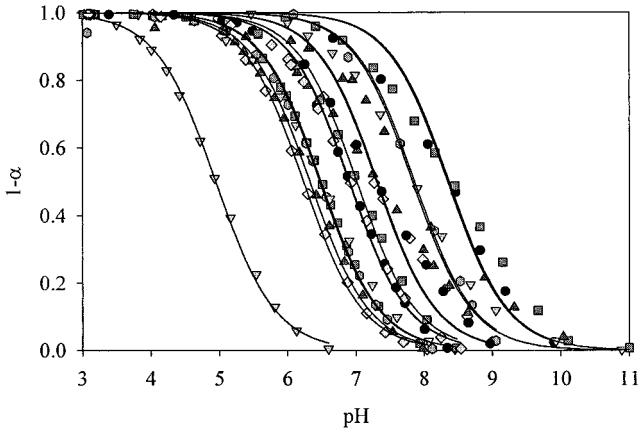

Figure 4. Degree of protonation (expressed by 1-α) as a function of pH in the combined buffer for the determination of ketocyanine basicities in TOPH-plastisized membranes. Solid lines represent the theoretical curve (eq 1) fitted to the experimental data. From left to right: calibration curves of chromoionophores 5ff, 5cd, 54c, 5ae, 5de, 5bd, 7bc, 5ab, 5bc, 5ce, 5ad, 5aa, 5ee, 5cc, 5dd, 5bb, and 5be.

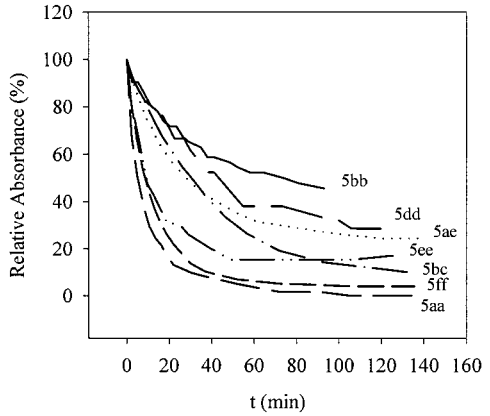

Figure 5. Representative curves of the decomposition study of the unprotonated ketocyanines in the TOPH−PVC membrane. Each dry membrane was directly exposed to a 500 W halogen lamp at 150 cm for 2 h at a temperature of 23 ± 2 °C. For comparison purposes, the initial absorbance of the deprotonated form at λ_{max} was set to 100%.

Stability. The loss of components due to chemical or photochemical processes is a limiting factor for optical sensors. Light is the most important cause of ketocyanine decomposition in routine work; therefore, the influence of different light sources at different conditions (humidity and air) was studied.

First of all, the combined effects of light (halogen lamp) and O_2 were evaluated in dry membranes. As was expected, they caused light-induced oxidation. The absorbance maxima of the spectrum decreased, and no decomposition products absorbing in the Vis−NIR range were present. Figure 5 shows the signal of each ketocyanine recorded along 2 h of exposition. The initial absorbance at the absorbance maximum was set to 100%. Calculated half-life times are summarized in Table 3. At first glance, results can be considered inadequate, because ketocyanines rapidly decompose under such conditions. For this reason, another photodecomposition test was carried out: the effect of monochromatic light at the absorbance maximum in the acid and basic form was studied in a mixed situation. The measuring cell was filled with the pH-adjusted solution until the dye was completely in the protonated or the deprotonated form. Then the flow cell was emptied to exclude leaching effects, and the membrane was irradiated. None of the ketocyanines suffered decomposition in the acid form during 2 h, but all of them slowly decomposed at their basic form (pH = 8), giving calculated half-life times over 20 h (Table 3). This study demonstrates that they were stable enough when calibrated in the usual laboratory conditions, and because the stability of the acid form was proved to be excellent, membranes were always conditioned at pH = 3 when stored.

Table 3. Half-Life and Absorbance Loss Percentage of Each Ketocyanine in Basic Conditions

dye	photostability ($h\nu^a + O_2$) $t_{1/2}$ (min)	chemical stability[b] % absorbance loss
5aa	6.86	0.1
5bb	76.35	0.7
5cc	15.37	2.4
5dd	57.07	
5ee	15.75	
5ff	9.86	0.5
5ab	13.51	1
5ac	12.29	1.9
5ad	10.15	1.0
5ae	40.16	0.7
5bc	31.52	3.0
5bd	10.42	0.5
5be	17.10	1.9
5cd	5.61	0.5
5ce	22.16	
5de	8.82	1.8
7bc	11.24	0.7

[a] Dry membranes were directly exposed to a halogen lamp (500 W) at 150 cm for 2 h. [b] Results are expressed as the percentage of the signal loss after 2 h in continuous flow conditions at pH 8.

Assuming that measurements are not carried out under intensive light and by proving that dyes do not aggregate in the membrane phase, the lipophilicity appears to be the factor that will determine the lifetime of an optode membrane. Therefore, the leaching rate was evaluated at pHs = 3 and 8. The tested ketocyanines appear to be stable in membrane under acidic conditions and did not leach, but spectra showed a slight decrease in the absorbance maxima under basic conditions. This attenuation was not attributed to a dye loss from the membrane, because the spectra of the sample solution did not exhibit the characteristic absorbance peaks of each dye. According to the verified effect of the sample pH in the stability of dyes during calibration curves, a chemical decomposition is assumed in such conditions. Table 3 shows that for all dyes, signal losses in basic conditions were not higher than 3% during the first 2 h and that membranes prepared with ketocyanines 5dd, 5ee, and 5cd were the most stable, because no losses of the signal were observed.

Analytical Response Characteristics. The analytical response characteristics were evaluated from successive calibration curves. An example of the obtained common calibration experiments in PVC membranes is presented in Figure 6. All of them gave the typical sigmoid curve, with the exception of the more basic dyes, which did not reach the signal saturation below pH = 8.5. Linear ranges covered two pH magnitude orders, and responses were fully reversible (if basicities did not exceed pH = 8.5) with a good reproducibility (RSD = 0.6−9%, n = 4). Moreover, there was no presence of hysteresis of the indicators

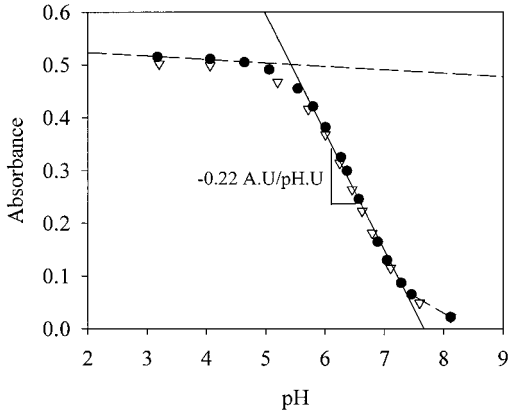

Figure 6. Calibration curve of the optode membrane containing dye 5ae, where the typical sigmoid response of the pH curves can be observed, and the slope of the linear range is shown. Every point was taken when the equilibrium was reached.

during all pH cycles. Sensitivities expressed as the slope of the calibration curve in the linear range are summarized in Table 4. Results demonstrated the high sensitivity of ketocyanine dyes.

All of the prepared and tested membranes can be considered very sensitive, fast, and reversible optical transducers, suitable for pH determinations.

The main problem in the miniaturization of optochemical sensors is the lack of sensitivity, because only reduced dye amounts can be incorporated into small-sized transducers. We have proved the suitability of ketocyanine dyes to improve sensitivity, but it is still possible to exploit their features by using them as the recognition reagents of integrated waveguide absorbance optodes (IWAOs) and then to provide miniaturized sensors with an enhanced performance.

Results Obtained with the IWAO. To validate this proposal, membranes of the same composition as in the conventional configuration were deposited onto the free propagation region of the devices to work out a comparative study.

Two representative calibration experiments obtained using both devices are shown in Figure 7a. As can be observed, the great advantage offered by the IWAO is the possibility of attaining high sensitivity without increasing the dye ratio or the membrane thickness. Figure 7b shows the good repeatability of the measurement, because values can be obtained with an acceptable relative standard deviation (pH = 6.07: 1.50 UA, RSD = 0.8%; pH = 7.08: 1.35 UA, RSD = 0.4%). Calculated sensitivities, as well as the slope of the calibration curve as the total absorbance changes between the fully protonated and deprotonated forms, are summarized in Table 4 for both experimental procedures. For comparison purposes, data obtained from the conventional configuration was collected at the absorbance maximum and at 780 nm, which is the wavelength of the LED source used in the IWAO. Results demonstrated that the new concept, on which the integrated sensor is based, allows acquisition of higher sensitivities using the same optically active reagents. Such an increase in sensitivity is due to the enlargement of the path length, but it is not constant for all of the tested dyes because of the shift between their absorbance maxima and the LED emission wavelength (780 nm). The slopes of the experimental calibration curves were at least doubled, multiplied by 28 with dye 5aa. Theoretically, the best results should be obtained with dyes whose absorbance maxima better match the wavelength of the LED source, but experimental results did not support this statement entirely. In any case, the signal rise is evident, and the effects that may alter response are being further studied.

To verify that the sensitivity increase is not related to the use of thicker membranes, response times were calculated for both configurations and then compared. Data showed that using the IWAO, the average of the response times calculated for every step change (usually 0.2 AU) were the same order as or lower than the ones obtained using the conventional configuration (Table 4). This fact led us to conclude that the membranes were at least the same thickness.

Table 4. Comparative Sensitivity and Response Time Results Obtained with the Conventional Configuration and the IWAO

		conventional configuration				IWAO		
dye	λ_{max} (nm)	slope[a] (λ_{max})	slope[a] (780 nm)	absorbance range[b] (780 nm)	t_r (min)	slope[a]	absorbance range[b]	t_r (min)
5aa	735.0	0.09	6×10^{-3}	0.014	3.6 ± 0.7	0.17	0.468	1.0 ± 0.3
5bb	766.0	0.03	0.02	0.079	2.2 ± 1.7	0.06	0.173	0.5 ± 0.2
5cc	765.0	0.06	0.02	0.059	3.0 ± 0.5	0.45	0.853	0.8 ± 0.2
5dd	764.0	0.16	0.10	0.228	1.0 ± 0.5			
5ee	768.5	0.19	0.19	0.739	3.6 ± 1.2	0.68	0.709	1.1 ± 0.3
5ff	727.0	0.27	5×10^{-3}	0.012	1.5 ± 0.2	0.09	0.064	1.2 ± 0.7
5ab	742.5	0.27	0.06	0.133	2.1 ± 0.5	0.10	0.329	1.0 ± 0.4
5ac	744.0	0.23	0.04	0.096	2.4 ± 0.7	0.51	1.020	0.9 ± 0.2
5ad	745.5	0.18	0.04	0.106	2.4 ± 0.5	0.24	0.633	2.7 ± 1.9
5ae	743.0	0.22	0.04	0.083	1.5 ± 0.5	0.40	0.911	1.0 ± 0.4
5bc	759.5	0.44	0.28	0.654	1.6 ± 0.2	0.68	2.062	1.6 ± 0.5
5bd	757.0	0.16	0.08	0.193	1.2 ± 1.1	0.65	1.437	0.7 ± 0.2
5be	766.0	0.16	0.04	0.106	1.5 ± 0.3	0.96	1.741	1.9 ± 0.4
5cd	755.0	0.06	0.03	0.060	2.0 ± 0.3	0.54	1.058	2.1 ± 0.8
5ce	770.5	0.18	0.14	0.424	1.3 ± 0.5	0.49	1.480	1.7 ± 0.5
5de	753.0	0.13	0.04	0.090	2.1 ± 0.4	0.35	0.646	0.8 ± 0.3
7bc	760.3	0.11	0.07	0.168	1.7 ± 0.6	0.30	1.001	0.7 ± 0.2

[a] Slopes are in absorbance units/pH units (a.u./pH u.). [b] The total absorbance range was taken at the same pH range for both configurations.

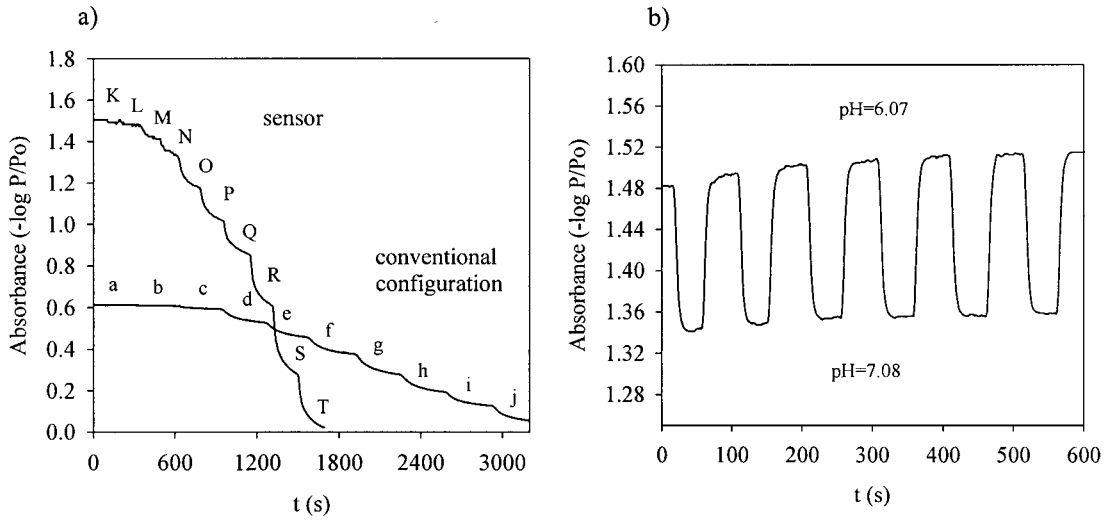

Figure 7. (a) Calibration experiments obtained with membranes containing dye 5ce in the conventional and new configuration at 780 nm. pH variations using the conventional configuration corresponded to (a) 3.09, (b) 4.04, (c) 5.10, (d) 6.17, (e) 6.64, (f) 7.07, (g) 7.59, (h) 8.04, (i) 8.40, and (j) 8.98. pH variations using the IWAO were (K) 3.14, (L) 5.09, (M) 5.99, (N) 6.44, (O) 6.97, (P) 7.29, (Q) 7.54, (R) 7.94, (S) 8.48, and (T) 8.98. (b) Short-time repeatability of the absorbance values at two different pHs using the sensor at 780 nm with the membrane containing dye 5ce.

To clarify the reason why it is possible to improve sensitivity without compromising response times, we want to mention again that, as a result of the planar configuration and the transmission of light perpendicular to the mass transfer, the sensitivity depends on the optical path length, but not on the membrane thickness.

CONCLUSIONS

Sensitive H^+-selective chromoionophores of different basicities in PVC membranes are presented. Their absorbance maxima are located in the NIR region, which is very appropriate for applications with telecommunication components. The prepared and characterized membranes showed a good analytical behavior. Hence, fully reversible, reproducible, fast, and sensitive bulk optodes were obtained. On the other hand, the IWAO proved to be a very promising alternative to the conventional optical sensors, as well as those based on fiber optics as the conventional flow-cell configuration.

Actually, the characterized dyes are being tested to develop integrated ion-selective optodes. The combination of the ketocyanine dyes with commercial ionophores will make the design of ion-selective optodes feasible, and the use of the IWAO will permit increasing sensitivity using simple and low-cost equipment so that analysis of a target analyte could be performed in different application fields.

ACKNOWLEDGMENT

The Spanish CICYT agency (through project no. TIC97-0594-C04-02) is greatly acknowledged for the financial support of the present work. we also thank Albert Montero for his work on the dye characterization.

Received for review July 16, 2001. Accepted October 18, 2001.

AC0107960